




Impacts of climate change on the state of Indiana: ensemble future projections based on statistical downscaling

Alan F. Hamlet¹  · Kyuhyun Byun¹ · Scott M. Robeson² · Melissa Widhalm³ · Michael Baldwin⁴

Received: 2 January 2018 / Accepted: 9 October 2018 / Published online: 2 January 2019
© Springer Nature B.V. 2019

Abstract

Using an ensemble of 10 statistically downscaled global climate model (GCM) simulations, we project future climate change impacts on the state of Indiana (IN) for two scenarios of greenhouse gas concentrations (a medium scenario—RCP4.5 and a high scenario—RCP 8.5) for three future time periods (2020s, 2050s, 2080s). Relative to a 1971–2000 baseline, the projections show substantial changes in temperature (T) for IN, with a change in the annual ensemble mean T for the 2080s RCP8.5 scenario of about 5.6 °C (10.1 °F). Such changes also indicate major changes in T extremes. For southern IN, the number of days with daily maximum T above 35 °C (95 °F) is projected to be about 100 days per year for the 2080s RCP8.5 scenario, as opposed to an average of 5 days for the historical baseline climate. Locations in northern IN could experience 50 days per year above 35 °C (95 °F) for the same conditions. Energy demand for cooling, as measured by cooling degree days (CDD), is projected to increase nearly fourfold in response to this extreme warming, but heating demand as measured by heating degree days (HDD) is projected to decline by 30%, which would result in a net reduction in annual heating/cooling energy demand for consumers. The length of the growing season is projected to increase by about 30 to 50 days by the 2080s for the RCP8.5 scenario, and USDA hardiness zones are projected to shift by about one full zone throughout IN. By the 2080s, all GCM simulations for the RCP8.5 scenario show higher annual precipitation (P) over the Midwest and IN. Projected seasonal changes in P include a 25–30% increase in winter and spring by the 2080s for the RCP8.5 scenarios and a 1–7% decline in summer and fall P (although there is a low model agreement in the latter two seasons). Rising T is projected to cause systematic decreases in the snow-to-rain ratio from Nov–Mar. Snow is projected to become uncommon in southern IN by the 2080s for the RCP8.5 scenario, and snowfall is substantially reduced in other areas of the state. The combined effects of these changes in T , P , and snowfall will likely result in increased surface runoff and flooding during winter and spring.

This article is part of a Special Issue on “The Indiana Climate Change Impacts Assessment” edited by Jeffrey Dukes, Melissa Widhalm, Daniel Vimont, and Linda Prokopy.

Electronic supplementary material The online version of this article (<https://doi.org/10.1007/s10584-018-2309-9>) contains supplementary material, which is available to authorized users.

✉ Alan F. Hamlet
hamlet.1@nd.edu

Extended author information available on the last page of the article

1 Introduction

Regional studies of climate change (CC) are instructive because of the expected consistency of impacts over similar geographical areas. States in the Midwestern region of the USA are a case in point and they are frequently analyzed together as a homogeneous region (e.g. Winkler et al. 2012; USGCRP 2017; Byun and Hamlet 2018). The Midwestern states, however, exhibit considerable variability in climate with both latitude and longitude. For example, the western and northern portions of the Midwest are considerably drier than the eastern and southern portions of the domain, and there are substantial increases in temperature from north to south.

In addition to better characterizing subregional heterogeneity, there is a need to provide CC information at scales that support *local* planning efforts and that facilitate meaningful engagement with diverse stakeholders whose interests are affected by climate. Urban planners in Minneapolis, Chicago, Indianapolis, and Cincinnati, for example, face similar kinds of problems related to CC that are affecting the Midwest as a whole (e.g., increases in extreme heat, humidity, and extreme precipitation), but the design of sustainable and resilient infrastructure in the four cities requires detailed CC projections that reflect the distinct baseline conditions for each city and the local effects of CC. One useful way to subset a region such as the Midwest, therefore, is to focus on climate change impacts at multiple administrative units, such as states, counties, and cities.

In this study, we provide CC projections at a fine spatial scale for the state of Indiana (IN) in the USA using statistically downscaled gridded data sets based on the Coupled Model Intercomparison Project, Phase 5 (CMIP5, Taylor et al. 2012) associated with the Intergovernmental Panel on Climate Change Fifth Assessment Report (IPCC AR5). This detailed statewide study supports the Indiana Climate Change Impacts Assessment (IN CCIA) (<http://www.purdue.edu/discoverypark/climate/in-ccia/>), led by the Purdue Climate Change Research Center, in partnership with the University of Notre Dame, Indiana University, the Midwestern Regional Climate Center, and Ball State University.

2 Regional climate change context

For the two most widely used greenhouse gas concentration scenarios, Representative Concentration Pathways (RCP) 4.5 and 8.5 (Moss et al. 2008) (representing “medium” and “high” twenty-first century greenhouse gas concentration trajectories respectively), the Midwestern United States is projected to experience profound changes in climate by 2100, especially for (T). Projections for annual mean T over the Midwestern United States from 31 global climate models (GCMs) for the RCP8.5 scenario show an ensemble mean increase in T of about 6.5 °C (11.7 °F) by 2100 relative to the historical 1971–2000 baseline (Fig. S1) (Byun and Hamlet 2018). The projected change in the annual ensemble mean T for RCP4.5 over the Midwestern United States is about 3.3 °C (5.9 °F) by 2100 relative to the 1971–2000 baseline. The upper tail of the annual mean T distribution, represented by the 97.5th percentile of the 31 GCM projections for RCP8.5 (i.e., a “worst-case” scenario), is nearly 10 °C (18 °F) warmer than the historical baseline by 2100. The change in ensemble mean T are for the Midwest is about 1.7 °C (3.1 °F) larger than the projected global average T increase over land reported by the IPCC (~4.8 °C (8.6 °F) by 2100 for RCP 8.5) (IPCC AR5 2013). As is apparent from Fig. S1, the signal-to-noise ratio for air temperature is very large, so detecting temperature shifts of this magnitude over time will not be difficult or ambiguous from a statistical perspective (Byun and Hamlet 2018). For example, by the 2050s, the 2.5th percentile of the GCM simulations is

already larger than the simulated 97.5th percentile for the mid-twentieth century climate. Consistent with results at the global scale (IPCC 2013), meaningful differences in annual air T between a “medium” (RCP 4.5) and “high” (RCP 8.5) emissions scenario are not evident until after the 2040s, suggesting that our collective ability to change T trajectories over the next 25 years may be minimal, even if concerted efforts are focused on reducing relatively short-lived greenhouse gasses such as methane or nitrous oxide (Smith and Mizrahi 2013). Changes in summer T show relatively little spatial variability across the Midwestern United States, whereas changes in winter T are largest in the northernmost and smallest in the southernmost parts of the domain (primarily due to snow-albedo and water-vapor feedbacks and differences in the relative importance of outgoing longwave radiation in winter) (Byun and Hamlet 2018). As a result, the existing latitudinal gradient in winter-mean T over the Midwest is projected to become less pronounced over time.

Annual precipitation (P) totals over the Midwest are projected to increase for all models by the 2080s for RCP 8.5, but the changes are most pronounced in winter (DJF) and spring (MAM) (Fig. S2). Mean changes in summer (JJA) and fall (SON), by comparison, are relatively small and the direction of change during these seasons is not consistent across the different GCM projections (Fig. S2; Byun and Hamlet 2018). In other words, the signal-to-noise ratio for projected P change is relatively high in winter and spring and relatively low in summer and fall. Even though these results are downscaled, it is important to note that GCMs, because of their coarse spatial resolution, currently are not able to explicitly capture changes in small-scale convective storms. As a result, some caution should be exercised in interpreting warm-season P statistics over IN, for which a substantial fraction of P is associated with small-scale convective storms. This also implies that, in assessing changes in summer P , the use of dynamical downscaling using high-resolution regional climate models is preferred due to the ability of such models to explicitly simulate convective storms in a physically based manner (see e.g., Liu et al. 2016; Prein et al. 2018). For similar reasons, we do not attempt to downscale GCM-simulated wind speed in this study.

We also note that there are some important linkages between changes in P and T , particularly in summer. It has been commonly found in past studies, for example, that the driest GCM scenarios in summer tend to also have the largest increases in T (see e.g., Rupp et al. 2013). We show in the results section below that this is also the case for IN, but that there are additional connections between strong warming and wetter conditions in the Midwest region.

3 Data and methods

3.1 Statistically downscaled CMIP5 climate projections

A comprehensive assessment of CC impacts in Indiana requires an integrated approach using several different kinds of observed data sets and downscaling approaches. Historical baselines for this study are provided by 1/16th degree latitude-longitude ($\sim 5 \times 7$ km) gridded meteorological data sets from 1915 to 2013 prepared over the Great Lakes and Midwestern states (Byun and Hamlet 2018). These historical data are corrected to account for precipitation gauge undercatch as a function of precipitation type (i.e., snow, mixed rain and snow, and rain) and wind speed. Statistical downscaling techniques used here are based on monthly GCM simulations and provide a range of expected results based on an ensemble of 10 GCM projections selected to capture the range of results from 31 different models (Byun and Hamlet 2018). As

used here, statistical downscaling facilitates an informed sensitivity analysis of the effects of changing climate on IN as a function of future greenhouse gas concentration scenarios.

Dynamical downscaling using high-resolution regional-scale climate models can provide physically based simulations of impacts that may not be adequately captured by statistical downscaling (e.g., interarrival time of storms, extreme wind, extreme humidity, precipitation from summer convective storms, and lake-effect snow). Dynamical downscaling, however, because of its much greater computational requirements, is often limited to the use of a single large-scale (global) forcing scenario, and therefore does not evaluate the range of GCM-derived uncertainty that statistical downscaling can more easily accommodate. In addition, after applying bias corrections based on observed probability distributions, statistical downscaling is particularly apt for evaluating projections of extreme T and P at fine spatial scales (Schoof and Robeson 2016; Byun and Hamlet 2018). Thus the two downscaling approaches complement each other by addressing different needs. For the remainder of this paper, however, we focus solely on results from statistical downscaling.

Climate change projections in this paper are evaluated using a suite of GCM simulations from the Coupled Model Intercomparison Project, Phase 5 (CMIP5; Taylor et al. 2012). Course-resolution GCM output is downscaled by the Hybrid Delta (HD) statistical downscaling approach (Hamlet et al. 2013; Tohver et al. 2014; Byun and Hamlet 2018) to 1/16th degree grid resolution ($\sim 5 \times 7$ km). As the name suggests, the HD is a hybrid approach combining monthly shifts in the T and P probability distributions derived from the well-known Bias Correction and Spatial Downscaling (BCSD) approach (Wood et al. 2002, 2004) with observed storm characteristics and accurate daily time series behavior (including extremes) deriving from gridded station observations. The HD approach produces a long time series of observed variability (1915–2013 in our case), superimposed on systematic changes in monthly probability distributions deriving from GCM simulations of future climate. Thus the HD future projections have the same sample size and essentially the same time series behavior as the historical baseline. A specific year, month, or day from the future time series can be directly compared to its historical counterpart (e.g., water year 1933 from the historical baseline can be directly compared to its future counterpart, water year “cc-1933”). These features of the HD make it very useful for calculating long-term climate statistics and estimating hydrometeorological extremes, because the historical and future products all have the same large sample size (99 years of daily data) and incorporate realistic storm and drought characteristics deriving from a long historical record. The strengths of the approach also imply some limitations, however, since the number of dry and wet days, the size and interarrival time of storms, and other contingent characteristics are inherited from the historical record and do not change in the future projections. Tohver et al. (2014), and Byun and Hamlet (2018) provide additional technical details on the HD approach.

For each greenhouse gas scenario, an ensemble of 10 GCM projections from the CMIP5 archive have been statistically downscaled for the 2020s (2011–2040), 2050s (2041–2070), and 2080s (2071–2100) using the HD approach over the entire Midwest region (Byun and Hamlet 2018). Methods used in selecting the 10 representative GCMs from a larger ensemble of 31 GCMs are reported in more detail by Byun and Hamlet (2018), but we give a brief overview here to help orient the reader. Using 31 GCMs from the CMIP5 archive, changes in annual T and P were calculated over the Midwest for the RCP 8.5 emissions scenario for the 2080s. The performance of the models in reproducing observed climate in the Midwest was also evaluated, and the models were ranked according to their performance. Three subsets of the GCM scenarios were then selected based on two separate criteria: (a) model performance (top half of the performance ranking) and (b) ability of the subset to capture the central tendency and

range of changes in T and P from the full ensemble. The first subset is a single model representing the central tendency of the entire 31-member ensemble. The second subset adds five models from the outer perimeter of the delta T and P space (total of six ensemble members). The third subset adds four additional members from an inner circle (total of 10 ensemble members) to strengthen sampling across the probability distribution (see Fig. 5 from Byun and Hamlet 2018). Although the subsets are constructed using annual changes in T and P , Fig. S2 shows that the 10-member ensemble also captures the range and central tendency of the full 31-member ensemble for different seasons reasonably well. For the analyses that we show in this paper, unless otherwise noted, the full 10-member ensemble is used.

The end products produced by the HD downscaling method are gridded daily data sets at 1/16th degree resolution that can be masked to produce summary results at a wide range of spatial scales including state- or county-wide averages, results for specific cities, or detailed statewide maps. In addition to the summary results produced for this paper, these data have been provided to several other working groups participating in the INCCIA to support their analyses, as reported in the other papers that make up this special issue.

3.2 Data processing methods for summary results

The analyses presented in this paper are based on three types of basic data processing techniques, which are outlined in Table 1. We will use abbreviated descriptions in figure captions to identify the method used to produce each figure. For example, Fig. 1 is a product

Table 1 Overview of data processing approaches used to generate figures and tables

	Overview of approach	Examples	Notes
Type I	Data are analyzed as a time series for each grid cell, and the results of the time series analysis (a single value for each cell) are then presented as a spatial map over some domain of interest.	Mean, variance, change relative to some base period, ratios of snow to P , extreme values, ensemble mean, etc. extracted from the time series for each cell and plotted as a map (color bar or contour plot).	In this paper, the domain of interest is mostly IN, but can be any subset of this domain.
Type II	Data are averaged in space for some domain of interest for each time step, and these single values for each time step are then plotted as a line graph with time in the X axis.	Domain average values of P or T plotted as an annual time series to show the effects of historical variability. Ranges can be shown by processing multiple GCMs as a separate time series and then statistically analyzing the ensemble at each time step (e.g., Fig. S1).	Any time step of interest can be used, but typically monthly or annual values are plotted.
Type III	Data are aggregated and/or averaged in space and time to produce a single value for each space/time data set. A single value may also be extracted for each calendar month, to produce a composite mean plot of the seasonal cycle.	Percent change in P for the Midwest for a group of GCMs to produce a range of values (e.g., Fig. S2). Monthly domain-average changes in T or P for a group of GCMs (e.g. Fig. 1).	

produced using Type III data processing, with data averaged in space over the entire domain (IN), and then presented as a composite mean plot.

4 Results and discussion

This section is divided into three main subsections, the first focusing on T and P impacts, the second focusing on impacts to growing-season length and U.S. Department of Agriculture (USDA) hardiness zones, and the third on impacts to heating and cooling degree days.

4.1 Summary of temperature and precipitation changes

4.1.1 Temperature changes

Similar to the rest of the Midwest and Great Lakes region, T -related impacts are expected to be substantial in Indiana (Fig. 1). By the mid-twenty-first century, T changes are more pronounced in summer than in winter. March and November show systematically lower amounts of warming than other months, and by the 2050s the largest temperature changes are in August. As expected, temperature changes are systematically larger for RCP 8.5 than for RCP 4.5 and increase with time for each greenhouse gas scenario (see also Fig. S1).

Spatial patterns of warming are somewhat dependent on season, but in general, there is relatively little spatial variability over IN. Table 2A summarizes the change in T for each time

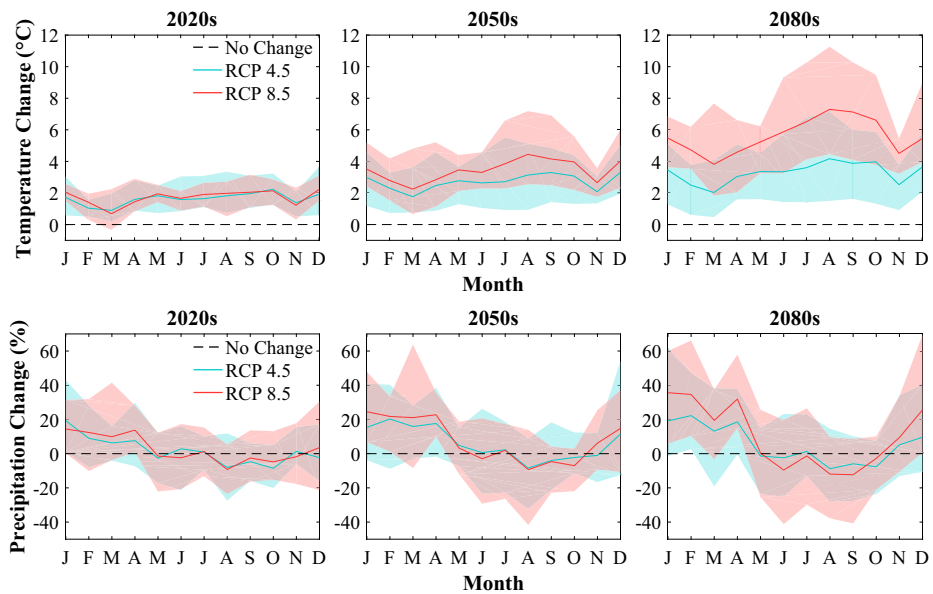


Fig. 1 Top panels: Monthly changes in T averaged over IN relative to a 1971–2000 baseline for the 2020s (2011–2040), 2050s (2041–2070), and 2080s (2071–2100) with ensemble range shown separately for two emissions scenarios (RCP4.5 and RCP8.5). Bottom panels: Monthly % changes in P relative to a 1971–2000 baseline with ensemble range for the 2020s, 2050s, 2080s RCP4.5 RCP8.5. [Method: type III, one value per calendar month averaged in time and space for each GCM scenario, and plotted as a range and central tendency for each month]

Table 2 (A) Projected annual and seasonal temperature changes (°C) over Indiana. The first value is the spatially averaged, ensemble mean temperature change. The value in parentheses is the spatial standard deviation of the ensemble mean delta T over Indiana. (B) Projected annual and seasonal precipitation changes (%) over Indiana. The first value is the spatially averaged, ensemble-mean, percent change in P . The value in parentheses is the spatial standard deviation over Indiana

A						
GHG scenarios	Future periods	Annual (°C)	Spring (°C)	Summer (°C)	Fall (°C)	Winter (°C)
RCP4.5	2020s	1.63 (0.10)	1.44 (0.11)	1.68 (0.10)	1.86 (0.10)	1.56 (0.11)
	2050s	2.71 (0.10)	2.34 (0.12)	2.83 (0.11)	2.82 (0.10)	2.86 (0.13)
	2080s	3.29 (0.11)	2.81 (0.11)	3.70 (0.11)	3.46 (0.12)	3.20 (0.14)
RCP8.5	2020s	1.73 (0.10)	1.36 (0.12)	1.85 (0.10)	1.80 (0.10)	1.89 (0.12)
	2050s	3.44 (0.11)	2.85 (0.12)	3.87 (0.12)	3.59 (0.11)	3.44 (0.17)
	2080s	5.60 (0.13)	4.54 (0.12)	6.56 (0.13)	6.08 (0.13)	5.22 (0.26)
B						
GHG scenarios	Future periods	Annual (%)	Spring (%)	Summer (%)	Fall (%)	Winter (%)
RCP4.5	2020s	1.78 (1.72)	3.75 (1.88)	-1.44 (1.84)	-3.89 (2.91)	8.69 (2.42)
	2050s	6.05 (1.67)	12.70 (1.81)	-1.83 (1.78)	-2.35 (3.34)	15.67 (2.71)
	2080s	5.33 (2.13)	10.15 (2.17)	-3.29 (2.11)	-2.72 (3.08)	17.20 (3.01)
RCP8.5	2020s	2.77 (1.74)	7.35 (1.70)	-3.45 (1.89)	-2.97 (3.29)	10.15 (2.48)
	2050s	7.70 (1.74)	15.67 (2.14)	-3.43 (1.89)	-1.76 (3.03)	20.33 (2.76)
	2080s	9.97 (2.07)	17.24 (2.52)	-7.60 (2.10)	-1.81 (2.98)	32.06 (2.99)

period and emissions scenario. Note that the spatial standard deviation of changes in T is much smaller than delta T for all seasons.

The annual number of frost days (days with $T_{min} < 0$ °C (32 °F)) in Indiana decreases steadily during the twenty-first century (Fig. 2), although there are still a relatively large number of frost days in winter even for the most extreme warming scenario investigated (2080s RCP8.5). Northern IN, for example, is projected to experience a 45% decrease in the number of frost days (from 135 per year for the baseline), but still has about 75 frost days per year on average even for the 2080s RCP8.5 scenario.

The number of days with extreme hot temperatures ($T_{max} > 35$ °C (95 °F)) in Indiana is projected to increase dramatically with warming (Fig. 3). By the 2080s, the RCP8.5 scenario shows extreme changes in the frequency of very hot days, especially in southern IN. In Evansville (in the southwest corner of the state), for example, the ensemble average number of very hot days increases to about 100 days per year from about 10 for the historical baseline climate. Table S1 shows the baseline and future projections of the number of extreme hot days for selected urban areas in Indiana. In northern IN, the ensemble mean number of extreme hot days increases to about 60 days per year on average for the 2080s RCP8.5 scenario from a historical baseline of about 3 days per year.

Although these projections point unambiguously to important T impacts in the Midwest and IN, there are some important caveats to be made. To begin with, an examination of historical trends in annual average T (Fig. S3) and the number of days with statewide average maximum T above 32.2 °C (90 °F) (Fig. S4) shows that natural climate variability in the twentieth century (and particularly the megadroughts of the Dust Bowl years in the 1930s and 1940s) has played an important role in determining annual average and extreme high T regimes in IN. The extreme drought conditions during the Dust Bowl years, for example, resulted in approximately 35 days per year with daily maximum T above 32.2 °C (90 °F). Since 1960, the average number of days above 32.2 °C has decreased to about 15 days per year on average, with no significant trend since 1960 (Fig. S4). One study (Mueller et al. 2016) has argued that increased evaporation due to changes in crops (increasing leaf area index and evapotranspiration) and increasing use of irrigation may have

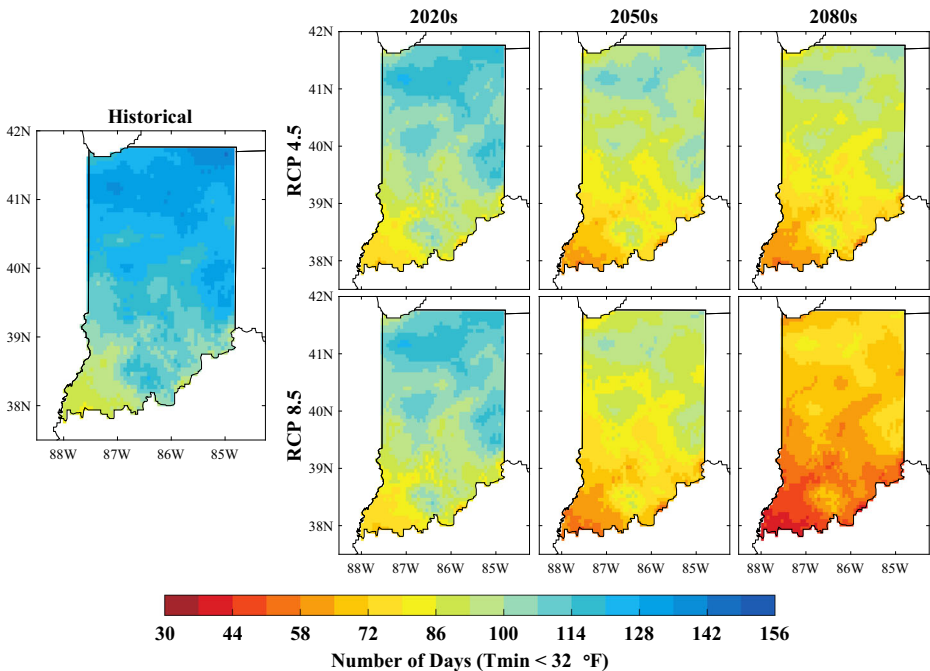


Fig. 2 Map of annual number of frost days ($T_{\min} < 0\text{ }^{\circ}\text{C}$ ($32\text{ }^{\circ}\text{F}$)). Seven panels: historical (1915–2013) and 2020s, 2050s, 2080s with RCP4.5 and RCP8.5 [Method: type I, ensemble mean annual number of frost days for each cell]

played a key role in the observed systematic shift in extreme summer temperatures, but this analysis excluded the Dust Bowl years and also data prior to 1910. An alternate explanation is simply that T feedbacks from increased P have been observed starting in about 1960 after several decades of very dry conditions. This better explains the available data from 1895 to 1915 shown in Fig. S3, for example, which show a similar average T regime to the post-1960 data, without the changes in crops and evaporation identified by Mueller et al. (2016).

Although land use, irrigation, and vegetation changes are not explicitly included in this study, linkages between drought cycles and T are present in the climate change projections, especially in summer. Figure S5 shows the relationship between delta T and delta P for the ensemble of 10 summer projections for three time periods and two greenhouse gas concentration scenarios. The analysis identifies two dominant and opposing relationships between delta T and delta P : one showing unusually dry conditions associated with warmer conditions, and the other showing wetter conditions associated with warmer conditions. The first relationship is most pronounced and consistent across different periods and concentration scenarios. Our hypothesis is that the first regime is related to increased solar radiation (reduced cloudiness) and systematic increases in the Bowen ratio (ratio of sensible to latent heat flux) that accompany low water availability at the land surface. The second relationship is likely caused by increased advection of warm and humid air from the Gulf of Mexico or the Atlantic coast, resulting in relatively warm and wet conditions. These results show that extreme summer heat in the future could be caused either by unusually dry summer conditions or by increased warm, moist air being advected into the region. It is clear, however, that the largest increases in T in summer accompany the driest scenarios, especially for

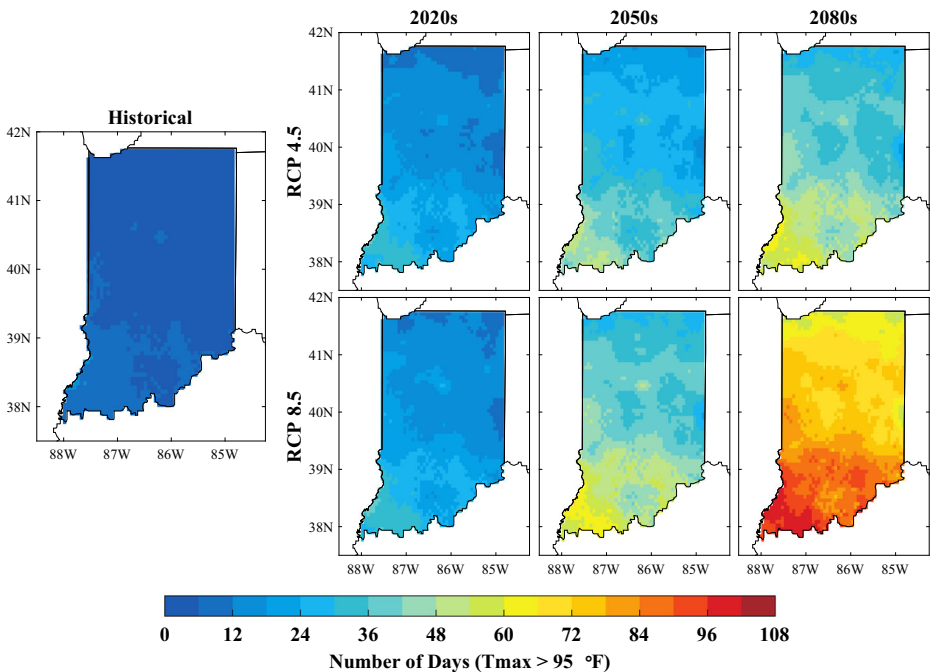


Fig. 3 Annual number of days with extreme hot temperatures ($T_{\max} > 35\text{ }^{\circ}\text{C}$ ($95\text{ }^{\circ}\text{F}$)). Seven panels: historical (1915–2013) and 2020s, 2050s, 2080s with RCP4.5 and RCP8.5 [Method: type I, ensemble mean number of extreme hot days]

the RCP8.5 2080s. For example, a reduction in summer precipitation on the order of 30% results in extreme warming of about $10\text{ }^{\circ}\text{C}$ in the projections, whereas scenarios with more modest reductions in P result in only about $5\text{ }^{\circ}\text{C}$ warming (Fig. S5).

Taken together, analysis of historical trends and future projections in daily maximum T suggest that extreme heat scenarios in IN could prove to be highly variable in time and may be linked to relatively uncertain summer P impacts. The relatively weak model agreement on summer P changes (Byun and Hamlet 2018), for example, suggests that impacts to summer P (and therefore extreme high temperatures) may vary substantially from decade to decade in response to natural climate variability, despite overall increases in average T . In an extreme case, a recurrence of extreme drought conditions like those experienced in the 1930s and 1940s could result in unprecedented, catastrophic heat impacts when coupled with the strong systematic warming in the future projections. Although this would appear to be a “worst-case” scenario, such extreme changes in P and T cannot be ruled out and could emerge without warning in just a few years’ time and then persist for several decades, as occurred during the Dust Bowl years (Fig. S4).

It is worth noting as well, that annual average T show similarly high values during the Dust Bowl years in the 1930s and 1940s, but also display significant increasing trends through time after 1960 (Fig. S3). Thus impacts to annual average T and daily maximum T extremes could prove to be quite different at different times in the future.

In addition to changing summer precipitation, atmospheric chemistry could play a role in suppressing increases in maximum daily temperatures (e.g., increasing particulate concentrations may increase albedo, resulting in net reductions in solar radiation). High-resolution

climate model simulations that include atmospheric chemistry are needed to explore these potential negative feedbacks on extreme high temperatures.

The number of extreme cold days ($T_{\min} < -15\text{ }^{\circ}\text{C}$ ($5\text{ }^{\circ}\text{F}$)) per year is projected to decrease with warming (Fig. S6). In the northern part of the domain, for example, the average number of extreme cold days per year declines from about 15 for baseline conditions to 5 for the 2080s RCP8.5 scenario. These changes will likely benefit IN via reductions in energy demand, decreased impacts to the transportation sector, etc.

4.1.2 Precipitation changes

For IN, P is projected to increase substantially in winter and spring for most scenarios (Fig. 1 bottom panels). Projected changes in summer and fall P , by comparison, show relatively small decreases and there is not a strong consensus between models for wetter or drier conditions in these seasons. This seasonal pattern of changing P increases in intensity through time in the scenarios. Projected annual changes in P are positive for almost all scenarios, and by the 2080s all GCMs show increases in annual P over the Midwest (Byun and Hamlet 2018) and IN.

At the macro scale, meaningful patterns of spatial variability for changes in P are not apparent, except during fall, which shows somewhat drier conditions in southern IN and wetter conditions in northern IN. Spring also shows a weak pattern of wetter conditions in the north, but all changes in P over IN are positive in this case. Note, however, that the spatial standard

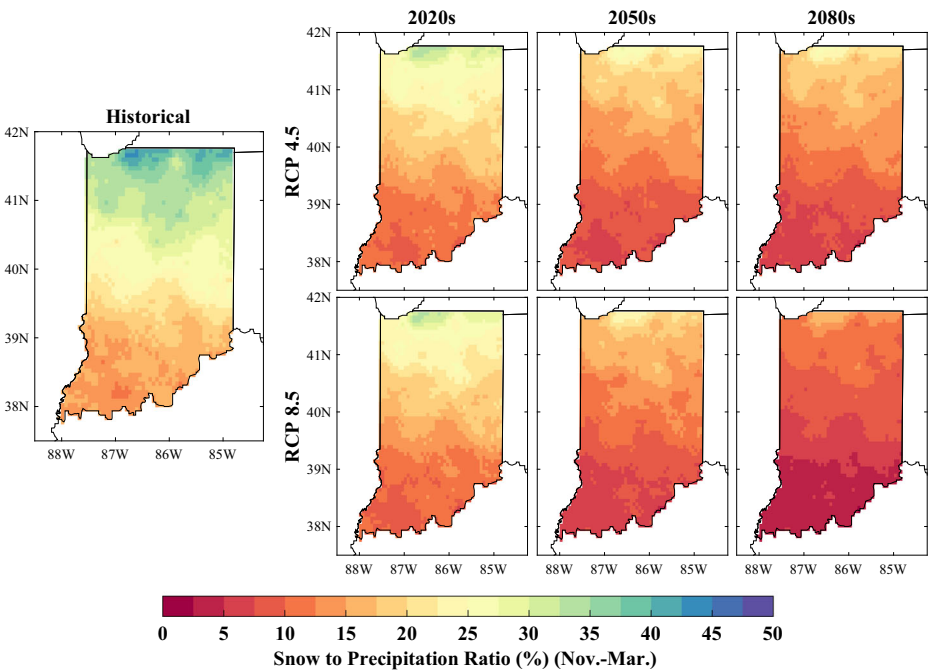


Fig. 4 Ensemble average, long-term-mean fraction of Nov–Mar P as snow. Seven panels: historical (1915–2013) and 2020s, 2050s, 2080s for the RCP4.5 and RCP8.5 emissions scenarios

deviation of delta P , calculated at the grid cell scale, is often comparable or larger in magnitude to the change in P itself. Table 2(B) summarizes percent changes in P for each season, emissions scenario, and time period.

Warming over the state is accompanied by a decreasing fraction of Nov–Mar P falling as snow (Fig. 4). By the 2080s for RCP8.5, snow is infrequent in southern IN (little snow even in midwinter), whereas northern IN still receives substantial snowfall from Nov–Mar, albeit much less snowfall during this period than for the historical baseline conditions.

Figure S7 shows substantial reductions in the number of P events with more than 5 mm of snow water equivalent (SWE), which is approximately equal to 5 cm (2 in.) of snowfall. This threshold was chosen because snowfall greater than this amount typically requires plowing to clear streets, and shoveling or snowblowing to clear sidewalks. This reduction in the number of days with more than 2 in. of snowfall implies fewer resources would be required for plowing (municipalities and businesses) and shoveling or snowblowing (individuals).

Although GCMs are not capable of explicitly simulating small-scale convective storms that are often associated with annual P extremes (see discussion of dynamical downscaling above), we nonetheless argue that simulations of heavy precipitation from GCMs, when coupled with quantile-based bias correction approaches, are likely to represent meaningful changes, especially in cool season when projected precipitation changes are largest and convective storms are relatively rare. Figure S8 shows increases in the ensemble average number of days per year with more than 25 mm of P . Some of the fine-scale patterns on the plot are caused by gridding artifacts (i.e., fewer extreme events are shown between stations due to averaging from multiple stations; Ensor and Robeson 2008), but the large-scale pattern nonetheless shows substantial increases of 3 to 4 days per year in the number of days of heavy precipitation. Analysis for a 50 mm P threshold (not shown) yielded qualitatively similar results. Results for selected urban centers in IN are shown in Table S2.

One caveat associated with this analysis is that the potential for increasing frequency of convective storms in mid-winter (e.g., on Feb 20, 2018, in IN) is not well captured in GCM simulations due to problems with spatial resolution. Similarly, changes in lake-effect snow, which are a function of both lake conditions (e.g., surface T , ice cover) and atmospheric conditions (e.g., frequency, intensity, and duration of arctic air outbreaks) are not well captured by GCMs, many of which do not even resolve the Great Lakes (Byun and Hamlet 2018). Simulations using high-resolution, regional-scale climate models coupled to lake hydrodynamic models are needed to better address changes in these two important impact pathways (Sharma et al. 2018).

4.2 Length of the frost-free growing season and USDA hardiness zone maps

The average length of the frost-free growing season increases substantially in the projected future climate (Fig. S9). By the 2020s, the length of the frost-free growing season increases by about 10 days overall and there are only minor differences between the RCP4.5 and 8.5 scenarios. By the 2080s, the RCP4.5 scenario shows increases in the growing season of 20 to 30 days whereas the RCP8.5 scenario shows increases of 30 to 50 days.

Changes in ensemble average USDA Plant Hardiness Zones (Fig. S10), which are based on expected extreme winter low T , show typical increases of about one full zone by the 2080s over much of IN, e.g., from zone 6a for the baseline climate to zone 7a for the 2080s RCP8.5 scenario. Note that the 7a zone indicated for northern IN for the 2080s RCP8.5 scenario is the

same hardiness zone as southern IN for the historical climate. Zone 7b, which currently occurs in northern Alabama, begins to appear in extreme southern Indiana in the 2080s RCP8.5 scenario.

4.3 Impacts to energy demand for space cooling and heating

Figure S11 and S12 show projected changes in cooling degree days ($^{\circ}\text{F}$) (relative to 75°F) and heating degree days (relative to 68°F) respectively. Cooling degree days increase by approximately a factor of 4 for the 2080s RCP8.5 scenarios, and heating degree days decline by about 30% for the same period and concentration scenario. These changes imply a net *decrease* in overall energy demand for space heating and cooling, however, due to the relatively large number of heating degree days in IN, and a typically higher coefficient of performance (COP) for electrical A/C equipment (COP ~ 2.5) as compared to electrical space heating (COP ~ 1.0) (see Raymond et al. 2018 and Hamlet et al. 2010 for additional discussion). Note that for heating degree days, the 2080s RCP8.5 values in northern IN are comparable to the historical values in southern IN; whereas, for cooling degree days, the 2080s RCP8.5 projections in northern IN are much higher than the historical values in southern IN. This difference reflects the fact that the largest T changes are projected during summer.

4.4 Constructing spatial analogs to IN's projected future climate

Spatial analogs for IN's projected future climate were constructed by finding the closest match for the projected future IN climate to the current climate in other parts of the country. These analogs were based on the gridded 1981–2010 mean T and P values from the PRISM data sets (Daly et al. 2008). For each PRISM grid-point, winter (DJF), and summer (JJA) means of T and P were used to find the minimum “distance” of the projected climate to the current climate using a six-element vector (T and P for each of the 3 months). Stratifying the data by winter and summer shows the distinct seasonal changes that are likely to occur in IN while allowing for closer spatial analogs to be found. Figures S13 and S14 show winter and summer analogs for the 2050s and 2080s, respectively for the two greenhouse gas concentration scenarios. In winter, IN's projected future climate approximates the current climate of the mid-Atlantic states (Fig. S13), whereas in summer IN's projected future climate approximates the current climate in areas substantially farther to the south and west (Fig. S14). By the 2080s for the RCP8.5 scenario, for example, IN's projected future climate in summer is comparable to the current climate of southeastern Texas.

5 Conclusions

The state of IN is projected to experience profound changes in climate by 2100. For the 2080s RCP8.5 climate change scenarios presented here, Indiana's climate will shift to one that is similar to the current climate for the mid-Atlantic states in winter and similar to the current climate of southeastern Texas in summer. Large changes in T are projected for IN, which will have major impacts on urban environments (Reynolds et al. 2018), human health (Filippelli et al. in review), energy (Raymond et al. 2018), agriculture (Bowling et al. in preparation), forests (Phillips et al. in review), and water resources (Cherkauer et al. in preparation). Substantial changes in traditional winter recreation opportunities are also projected due to systematic loss

of snow and ice cover in the future (Chin et al. 2018). Changes in extreme high T are most clearly linked to drought in both the historical record and future projections, which implies that impacts to extreme high T may be quite variable in time in response to relatively uncertain changes in summer P in the projections. That is, unusually dry decades in the future may show extreme heat impacts, whereas less drought-prone decades may be substantially cooler. Unusually wet conditions in summer are also associated with very warm conditions in the projections, however, which suggest that warm, moist air advected from the south may be another important cause of extreme heat and humidity in the projections.

Reductions in energy demand for space heating due to warming, however, will likely be a benefit to many (see also Raymond et al. 2018), and reductions in snowfall may reduce costs of snow removal for municipalities, businesses, and individuals. Projected changes in P , particularly its seasonality, are also substantial, with a projected 25–30% increase in winter and spring P by the 2080s for the RCP8.5 scenario. By the 2080s all climate models in the RCP8.5 CMIP5 archive show increases in annual P over IN, but increasing evapotranspiration with warming could reduce the net effects on soil moisture (Cherkauer et al. in preparation). Changes in summer convective storms cannot be captured by large-scale climate models like the ones used in this study, but increasing P intensity from convective storms has already emerged in the historical record as an important impact pathway for cities and these trends are projected to continue to increase with future warming (e.g., Prein et al. 2018). We also hypothesize that convective storms will be increasingly observed in winter as warming progresses. Coincident increases in P as rain, accompanied by loss of snow cover in winter and spring, will likely impact water quality and erosion in agricultural areas (Bowling et al. in preparation) and may lead to elevated soil moisture and increased flooding in winter and spring in IN rivers (Cherkauer et al. in preparation; Byun et al. 2019). Lake-effect snow is hypothesized to increase in the next several decades due to warmer lake surface temperatures and longer ice-free conditions, but towards the end of the twenty-first century T may become too warm, resulting in conversion from lake-effect snow to lake-effect rain, especially in the shoulder seasons. Regional-scale climate models dynamically coupled to lake hydrodynamic models are needed to evaluate these impact pathways in a more physically based manner.

Acknowledgements This paper is a contribution to the Indiana Climate Change Impacts Assessment (INCCIA). The INCCIA is organized and financially supported by the Purdue Climate Change Research Center.

Publisher's Note Springer Nature remains neutral with regard to jurisdictional claims in published maps and institutional affiliations.

References

- Byun K, Hamlet AF (2018) Projected changes in future climate over the Midwest and Great Lakes region using downscaled CMIP5 Ensembles. *Int J Climatol* 38:e531–e553. <https://doi.org/10.1002/joc.5388>
- Byun K, Chiu CM, Hamlet AF (2019) Effects of 21st century climate change on seasonal flow regimes and hydrologic extremes over the Midwest and Great Lakes region of the US. *Science of The Total Environment* 650:1261–1277. <https://doi.org/10.1016/j.scitotenv.2018.09.063>
- Chin N, Byun K, Hamlet AF, Cherkauer KA (2018) Assessing potential winter weather response to climate change and implications for tourism in the U.S. Great Lakes and Midwest. *Journal of Hydrology: Regional Studies* 19:42–56. <https://doi.org/10.1016/j.ejrh.2018.06.005>

- Daly C, Halbleib M, Smith JI, Gibson WP, Doggett MK, Taylor GH, Curtis J, Pasteris PP (2008) Physiographically sensitive mapping of climatological temperature and precipitation across the conterminous United States. *Int J Climatol* 28:2031–2064. <https://doi.org/10.1002/joc.1688>
- Ensor LA, Robeson SM (2008) Statistical characteristics of daily precipitation: comparisons of gridded and point datasets. *J Appl Meteorol Climatol* 47(9):2468–2476
- Hamlet AF, Lee SY, Mickelson KEB, Elsner MM (2010) Effects of projected climate change on energy supply and demand in the Pacific Northwest and Washington State. *Clim Chang* 102(1–2). <https://doi.org/10.1007/s10584-010-9857-y>
- Hamlet AF, Elsner MM, Mauger G, Lee S-Y, Tohver I, Norheim RA (2013) An overview of the Columbia Basin Climate Change Scenarios Project: approach, methods, and summary of key results. *Atmosphere-Ocean* 51: 392–415. <https://doi.org/10.1080/07055900.2013.819555>
- IPCC, 2013, Climate Change 2013: The physical basis. Contribution of Working Group 1 to the Fifth Assessment Report of the IPCC, Cambridge University Press, 1535pp
- Liu C, Ikeda K, Rasmussen R, Barlage M, Newman AJ, Prein AF, Chen F, Chen L, Clark M, Dai A, Dudhia J (2016) Continental-scale convection-permitting modeling of the current and future climate of North America. *Clim Dyn*:1–25
- Moss, R.; Mustafa Babiker; Sander Brinkman; Eduardo Calvo; Tim Carter; Jae Edmonds; Ismail Elgizouli; Seita Emori; Lin Erda; Kathy Hibbard; Roger Jones; Mikiko Kainuma; Jessica Kelleher; Jean Francois Lamarque; Martin Manning; Ben Matthews; Jerry Meehl; Leo Meyer; John Mitchell; Nebojsa Nakicenovic; Brian O'Neill; Ramon Pichs; Keywan Riahi; Steven Rose; Paul Runci; Ron Stouffer; Detlef van Vuuren; John Weyant; Tom Wilbanks; Jean Pascal van Ypersele & Monika Zurek, 2008: Towards new scenarios for analysis of emissions, climate change, impacts, and response strategies, Geneva: intergovernmental panel on Climate Change. p. 132
- Mueller ND, Butler EE, McKinnon KA, Rhines A, Tingley M, Holbrook NM, Huybers P (2016) Cooling of US Midwest summer temperature extremes from cropland intensification. *Nat Clim Chang* 6(3):317–322
- Prein AF, Liu C, Ikeda K, Trier SB, Rasmussen RM, Holland GJ, Clark MP (2018) Increased rainfall volume from future convective storms in the US. *Nat Clim Chang* (7):880–884
- Raymond L, Gotham D, McClain W, Mukherjee S, Nateghi R, Preckel PV, Schubert P, Singh S, Wachs L Projected climate change impacts on Indiana's energy demand and supply. *Climatic Change* (in press)
- Rupp DE, Abatzoglou JT, Hegewisch KC, Mote PW (2013) Evaluation of CMIP5 20th century climate simulations for the Pacific Northwest USA. *J Geophys Res Atmos* 118(10):884–10,906. <https://doi.org/10.1002/jgrd.50843>
- Schoof JT, Robeson SM (2016) Projecting changes in regional and local climate extremes in the United States. *Weather and Climate Extremes* 11:28–40
- Sharma A, Hamlet AF, Fernando HJS, Catlett CE, Horton DE, Kotamarthi VR, Kristovich DAR, Packman AI, Tank JL, Wuebbles DJ (2018) The Need for an Integrated Land-Lake-Atmosphere Modeling System, Exemplified by North America's Great Lakes Region. *Earth's Future* 6(10):1366–1379. <https://doi.org/10.1029/2018EF000870>
- Smith SJ, Mizrahi A (2013) Near-term climate mitigation by short-lived forcers. *Proc Natl Acad Sci* 110(35): 14202–14206
- Taylor KE, Stouffer RJ, Meehl GA (2012) An overview of CMIP5 and the experiment design. *Bull Am Meteorol Soc* 93:485–498. <https://doi.org/10.1175/BAMS-D-11-00094.1>
- Tohver IM, Hamlet AF, Lee SY (2014) Impacts of 21st-century climate change on hydrologic extremes in the Pacific Northwest Region of North America. *J Am Water Resour Assoc* 50:1461–1476. <https://doi.org/10.1111/jawr.12199>
- USGCRP (2017) In: Wuebbles DJ, Fahey DW, Hibbard KA, Dokken DJ, Stewart BC, Maycock TK (eds) Climate science special report: fourth national climate assessment, volume I. U.S. Global Change Research Program, Washington, DC, p 470
- Winkler JA, Arriitt RW, Pryor SC (2012) Climate projections for the Midwest: availability, interpretation and synthesis. *US Natl Clim Assess Midwest Tech Input Rep* 24:9781610915113
- Wood AW, Maurer EP, Kumar A, Lettenmaier DP (2002) Long range experimental hydrologic forecasting for the eastern U.S. *J Geophys Res* 107(D20):4429. <https://doi.org/10.1029/2001JD000659>
- Wood AW, Leung LR, Sridhar V, Lettenmaier DP (2004) Hydrologic implications of dynamical and statistical approaches to downscaling climate model outputs. *Clim Chang* 62:189–216. <https://doi.org/10.1023/B:CLIM.0000013685.99609.9c>

Affiliations

Alan F. Hamlet¹ · Kyuhyun Byun¹ · Scott M. Robeson² · Melissa Widhalm³ · Michael Baldwin⁴

¹ Department of Civil and Environmental Engineering and Earth Sciences, University of Notre Dame, Notre Dame, IN 46556, USA

² Department of Geography, Indiana University Bloomington, Bloomington, IN 47405, USA

³ Climate Change Research Center, Purdue University, West Lafayette, IN 47907, USA

⁴ Department of Earth, Atmospheric, and Planetary Sciences, Purdue University, West Lafayette, IN 47907, USA